1-23-2017

Inelastic Neutron Scattering Cross Section Measurements for ^{134,136}Xe of Relevance to Neutrinoless Double-β Decay Searches

Erin E. Peters
University of Kentucky, fe.peters@uky.edu

T. J. Ross
University of Kentucky

S. H. Liu
University of Kentucky

Marcus T. McEllistrem
University of Kentucky, marcusmcellistrem@uky.edu

Steven W. Yates
University of Kentucky, yates@uky.edu

Inelastic Neutron Scattering Cross Section Measurements for ^{134,136}Xe of Relevance to Neutrinoless Double-β Decay Searches

Notes/Citation Information
Published in *Physical Review C*, v. 95, issue 1, 014325, p. 1-4.

Digital Object Identifier (DOI)
https://doi.org/10.1103/PhysRevC.95.014325

Inelastic neutron scattering cross section measurements for ^{134,136}Xe of relevance to neutrinoless double-β decay searches

E. E. Peters,[1,*] T. J. Ross,[1,2] S. H. Liu,[1,2] M. T. McEllistrem,[2] and S. W. Yates[1,2]
[1]*Department of Chemistry, University of Kentucky, Lexington, Kentucky 40506-0055, USA*
[2]*Department of Physics & Astronomy, University of Kentucky, Lexington, Kentucky 40506-0055, USA*
(Received 13 September 2016; revised manuscript received 4 December 2016; published 23 January 2017)

Neutrinoless double-β decay ($0\nu\beta\beta$) searches typically involve large-scale experiments for which backgrounds can be complex. One possible source of background near the $0\nu\beta\beta$ signature in the observed spectra is γ rays arising from inelastic neutron scattering from the materials composing or surrounding the detector. In relation to searches for the $0\nu\beta\beta$ of ^{136}Xe to ^{136}Ba, such as the EXO-200 and KamLAND-Zen projects, inelastic neutron scattering γ-ray production cross sections for ^{136}Xe and ^{134}Xe are of importance for characterizing such γ rays that may inhibit the unambiguous identification of this yet-to-be-observed process. These cross sections have been measured at the University of Kentucky Accelerator Laboratory at neutron energies from 2.5 to 4.5 MeV.

DOI: 10.1103/PhysRevC.95.014325

I. INTRODUCTION

The observation of neutrinoless double-β decay $0\nu\beta\beta$ promises to be the best way to establish the absolute mass of the neutrino and to determine whether neutrinos are Majorana particles, i.e., their own antiparticles. Two-neutrino double-β decay has been observed for many nuclei—^{48}Ca, ^{76}Ge, ^{82}Se, ^{96}Zr, ^{100}Mo, ^{116}Cd, ^{128}Te, ^{130}Te, ^{136}Xe, ^{150}Nd, and ^{238}U [1], but $0\nu\beta\beta$ has not. Several of these isotopes are the subjects of searches for $0\nu\beta\beta$ in large-scale experiments, such as ^{76}Ge in the Majorana [2] and GERDA [3] projects and ^{136}Xe in the EXO-200 [4] and KamLAND-Zen [5] experiments. The signature for $0\nu\beta\beta$ is a discrete signal corresponding to the energy of the Q value of the decay, which for the decay of ^{136}Xe to ^{136}Ba is 2457.99(27) keV [6]. Critical to these large-scale experiments is an understanding of backgrounds which may produce a signal resembling a $0\nu\beta\beta$ event and complicate the unambiguous identification of this process. Methods have been developed in order to reduce the impact of such background events. For example, the EXO-200 Collaboration employs a muon detection system to actively veto most muon-induced events [4]. EXO-200 also possesses the ability to distinguish between single-site and multisite events. In a single-site event, all charges are deposited within a single volume with dimensions of 2 to 3 mm; all other events are considered multisite [4]. Charged-particle interactions tend to be single-site, whereas γ-ray interactions are predominantly multisite due to Compton scattering.

A possible source of background that may be difficult to distinguish arises from inelastic neutron scattering (INS). Neutrons are produced by natural radioactivity in the surroundings as well as by incident muons. These neutrons may then inelastically scatter from the detector or neighboring materials populating excited states in these nuclei and potentially emitting γ rays with energies in the region of interest (ROI) near the Q value. It is, therefore, important to identify such γ rays and measure INS γ-ray production cross sections for the nuclei composing the detector components. Both the EXO-200 and the KamLAND-Zen experiments incorporate enriched Xe—80.6% ^{136}Xe and 19.4% ^{134}Xe for EXO-200 [7] and 90.9% ^{136}Xe and 8.9% ^{134}Xe for KamLAND-Zen [5]. Although γ-ray production cross sections for neutron scattering from structural materials are also important, the materials producing backgrounds can be eliminated or their use reduced. The cross sections of ^{134,136}Xe are the present subjects of study.

II. EXPERIMENTS

At the University of Kentucky Accelerator Laboratory (UKAL), nearly monoenergetic neutrons ($\Delta E \approx 50$ keV) were produced by the ^{3}H$(p,n)^3$He reaction using accelerated protons from the 7-MV Van de Graaff accelerator incident upon a cell of tritium gas at a pressure of approximately 1 atm. The gas cell was separated from the beamline by a 3.6-μm molybdenum foil. The resultant neutrons were scattered from highly enriched ($>99.9\%$) samples of solid ^{134}XeF$_2$ (11.50 g) and ^{136}XeF$_2$ (10.65 g) contained in polytetrafluoroethylene vials with an inner diameter of 1.8 cm. Subsequent γ rays were detected using a bismuth germanate (BGO) Compton-suppressed HPGe detector of $\approx 50\%$ relative efficiency. γ-ray spectra were obtained for incident neutron energies of 2.5–4.5 MeV in 0.25-MeV increments at a detection angle of 125° in order to minimize the effects of the angular distribution of the emitted γ rays when a Legendre polynomial fit of the form $W(\theta) = A_0[1 + A_2P_2(\cos\theta) + A_4P_4(\cos\theta)]$ is applied. Spectra also were obtained for a 59.23-g metallic cylinder of natural iron 1.90 cm in diameter and 2.54 cm in height at each neutron energy in order to measure the yield of the 847-keV γ ray of ^{56}Fe such that the INS γ-ray production cross section may be used as a standard.

III. ANALYSIS AND RESULTS

Cross sections were determined by obtaining the yield of each γ ray in ^{134,136}Xe as well as the 847-keV γ ray in ^{56}Fe at each incident neutron energy and correcting for the efficiency of the detector, multiple scattering of neutrons, and γ-ray absorption within the sample. The detector efficiency was

*fe.peters@uky.edu

TABLE I. INS cross sections for γ rays in ^{134}Xe within the ROI for $E_n = 2.5$–4.5 MeV. E_γ is in keV, and σ_{E_n} is in millibarns.

E_γ	$\sigma_{2.5}$	$\sigma_{2.75}$	$\sigma_{3.0}$	$\sigma_{3.25}$	$\sigma_{3.5}$	$\sigma_{3.75}$	$\sigma_{4.0}$	$\sigma_{4.25}$	$\sigma_{4.5}$
2407.7					3.02(66)	4.78(94)	4.87(76)	4.36(86)	4.54(99)
2418.6					4.20(73)	6.8(10)	6.07(82)	5.26(89)	4.89(97)
2452.9					1.95(60)	3.02(79)	3.13(64)	3.75(81)	3.52(89)
2465						1.40(84)	1.63(57)		
2467.6					2.62(62)	3.14(92)	5.14(78)	5.93(94)	5.7(10)
2477.5					1.37(56)	3.78(84)	3.59(68)	2.77(77)	2.55(85)
2485.7	0.90(39)	10.8(10)	13.2(12)	16.5(14)	16.9(15)	18.4(18)	14.0(13)	11.2(13)	10.6(14)
2490.7					1.93(59)	4.51(89)	4.22(70)	4.72(89)	3.10(86)
2506.6						2.91(77)	2.10(56)	2.46(74)	

TABLE II. INS cross sections for γ rays in ^{136}Xe within the ROI for $E_n = 2.5$–4.5 MeV. E_γ is in keV, and σ_{E_n} is in millibarns.

E_γ	$\sigma_{2.5}$	$\sigma_{2.75}$	$\sigma_{3.0}$	$\sigma_{3.25}$	$\sigma_{3.5}$	$\sigma_{3.75}$	$\sigma_{4.0}$	$\sigma_{4.25}$	$\sigma_{4.5}$
2414.8	30.0(22)	88.1(59)	114.8(76)	148.1(99)	155(10)	162(11)	139.4(96)	134.6(93)	111.8(82)
2480							3.31(78)	4.28(94)	5.5(13)
2498.5							3.76(79)	9.1(13)	9.9(16)

TABLE III. INS cross sections for levels in ^{134}Xe with energies within the ROI for $E_n = 2.5$–4.5 MeV. E_{level} is in keV, and σ_{E_n} is in millibarns.

E_{level}	$\sigma_{2.5}$	$\sigma_{2.75}$	$\sigma_{3.0}$	$\sigma_{3.25}$	$\sigma_{3.5}$	$\sigma_{3.75}$	$\sigma_{4.0}$	$\sigma_{4.25}$	$\sigma_{4.5}$
2408.6	5.87(87)	18.4(14)	30.0(20)	43.7(28)	53.5(34)	65.5(42)	59.4(38)	66.2(43)	71.0(45)
2440.4	9.90(88)	30.7(22)	37.8(27)	44.3(31)	38.5(28)	45.2(34)	37.3(28)	36.9(28)	32.1(41)
2485.7	2.67(56)	40.6(20)	51.6(25)	66.6(31)	69.7(33)	72.9(37)	57.5(29)	47.5(34)	43.6(34)
2502.4		32.6(17)	47.8(23)	63.1(29)	70.6(33)	78.3(39)	67.4(33)	71.8(36)	72.3(37)

TABLE IV. INS cross sections for levels in ^{136}Xe with energies within the ROI for $E_n = 2.5$–4.5 MeV. E_{level} is in keV, and σ_{E_n} is in millibarns.

E_{level}	$\sigma_{2.5}$	$\sigma_{2.75}$	$\sigma_{3.0}$	$\sigma_{3.25}$	$\sigma_{3.5}$	$\sigma_{3.75}$	$\sigma_{4.0}$	$\sigma_{4.25}$	$\sigma_{4.5}$
2414.8	32.5(31)	96.0(61)	124.1(77)	159(10)	169(11)	177(11)	149.9(98)	145.9(95)	119.5(84)
2444.4	3.39(55)	18.3(14)	33.8(21)	63.5(35)	96.5(52)	100.3(56)	105.0(59)	112.7(62)	115.1(65)
2465.1	8.63(89)	35.1(23)	69.8(41)	101.3(59)	134.2(79)	154.2(91)	135.6(81)	146.9(87)	135.1(84)

TABLE V. Selected portion of the level scheme for ^{134}Xe. Energies are given in keV. Levels and γ rays in bold font were observed for the first time in the INS measurements. B.R. is the γ-ray branching ratio.

$E_{\text{level}_{\text{initial}}}$	E_γ	$E_{\text{level}_{\text{final}}}$	B.R.
847.1	847.1	0.0	1
1613.8	766.7	847.1	0.501(9)
	1613.8	0.0	0.499(9)
1731.2	884.2	847.1	1
1919.7	188.5	1731.2	0.033(3)
	1072.6	847.1	0.967(15)
2408.6	488.9	1919.7	0.129(15)
	677.4	1731.2	0.871(40)
2440.4	**1593.4**	847.1	1
2485.7	**871.8**	1613.8	0.286(24)
	1638.6	847.1	0.464(28)
	2485.7	0.0	0.250(21)
2502.4	**771.1**	1731.2	0.518(25)
	888.5	1613.8	0.269(19)
	1655.3	847.1	0.213(18)

determined using ^{226}Ra and ^{56}Co sources. Multiple scattering corrections were calculated using an in-house code based on the work of Engelbrecht [8] for inelastic scattering from cylindrical samples. The corrected yields were then used to calculate the ^{134,136}Xe γ-ray production cross sections relative to those for ^{56}Fe taken from Ref. [9]. For neutron energies which are between those presented in Ref. [9], a linear interpolation was applied. The cross sections for individual γ rays with energies in the ROI, i.e., within a 100-keV window centered on the end-point energy of 2458 keV, are presented in Tables I and II for ^{134}Xe and ^{136}Xe, respectively. Spectra showing this region for both nuclei are displayed in Figs. 1 and 2; excitation functions for the two most intense γ rays in the region of interest are shown in Figs. 3 and 4: the 2486-keV γ ray in ^{134}Xe and the 2415-keV γ ray in ^{136}Xe, respectively.

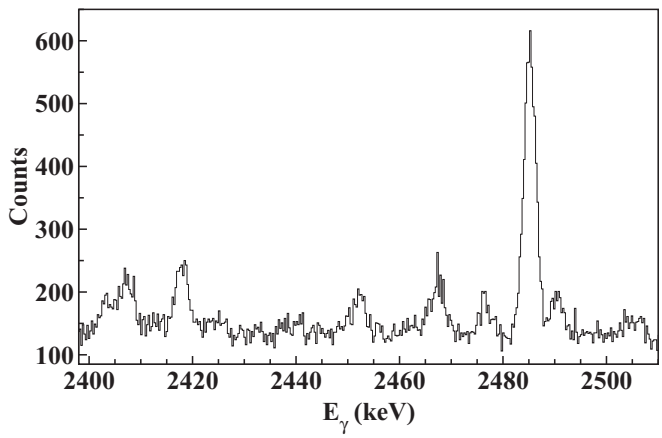

FIG. 1. Summed spectrum of the data obtained at all incident neutron energies for ^{134}Xe illustrating γ rays in the ROI.

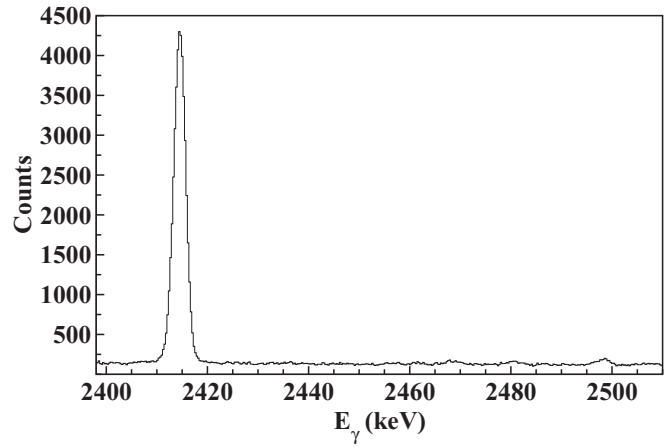

FIG. 2. Summed spectrum of the data obtained at all incident neutron energies for ^{136}Xe illustrating γ rays in the ROI.

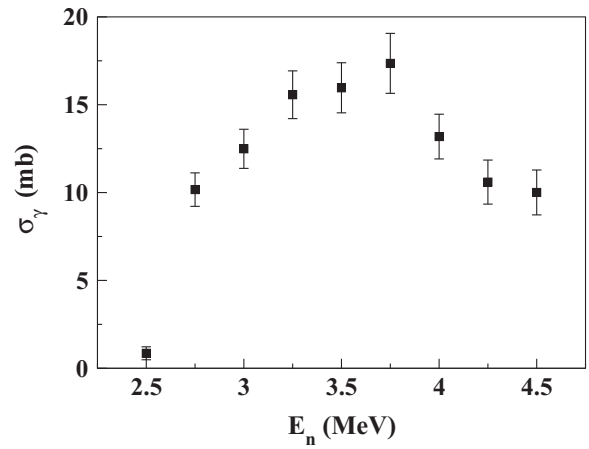

FIG. 3. Cross section as a function of incident neutron energy for the 2486-keV γ ray in ^{134}Xe.

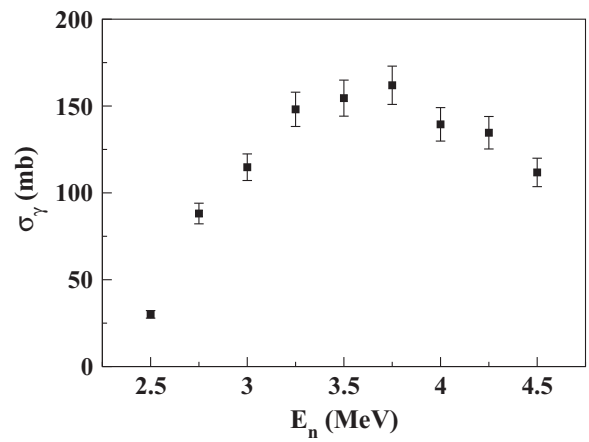

FIG. 4. Cross section as a function of incident neutron energy for the 2415-keV γ ray in ^{136}Xe.

TABLE VI. Selected portion of the level scheme for ^{136}Xe. Energies are given in keV. B.R. is the γ-ray branching ratio.

$E_{\text{level}_{\text{initial}}}$	E_γ	$E_{\text{level}_{\text{final}}}$	B.R.
1313.1	1313.1	0.0	1
1694.4	381.4	1313.1	1
1891.6	197.2	1313.1	1
2125.7	431.3	1694.4	0.198(6)
	812.6	1313.1	0.802(15)
2261.7	370.1	1891.6	1
2414.8	1101.5	1313.1	0.077(9)
	2414.8	0.0	0.923(30)
2444.4	182.7	2261.7	0.061(12)
	318.5	2125.7	0.079(12)
	552.5	1891.6	0.107(12)
	750.0	1694.4	0.753(31)
2465.1	339.3	2125.7	0.132(9)
	770.6	1694.4	0.868(23)

The cross sections for levels with energies in the ROI are also of interest as cascades of γ rays from the level to the ground state sum to energies in the ROI and may be detected as multisite events. These values were calculated by summing the γ-ray cross sections for all branches and are given in Tables III and IV. In order to calculate the probability that a given cascade would occur, information about the level scheme is required. Relevant levels, γ rays, and branching ratios obtained by taking a weighted average of the branching ratios calculated separately for each incident neutron energy are presented in Tables V and VI. One noteworthy exception to this procedure concerns the 2486-keV level in ^{134}Xe. The 1639-keV γ ray is an unresolved doublet in the 4.25- and 4.50-MeV spectra, evident by broadening of the peak and an increase in its calculated branching ratio. For these two incident neutron energies, the cross section for the 1639-keV γ ray was determined using the average branching ratios for incident neutron energies from 2.75 to 4.0 MeV and the γ-ray cross section of the 2486-keV γ ray. The level cross section is a sum of the γ-ray cross sections for all three branches.

IV. CONCLUSIONS

The measured γ-ray production cross sections for ^{134,136}Xe from inelastic neutron scattering are given in Tables I and II. Level population cross sections are presented in Tables III and IV. Of particular interest are the 2415-keV ground-state γ ray in ^{136}Xe with a cross section of $\approx$120 mb and the 2486-keV ground-state γ ray in ^{134}Xe with a cross section of $\approx$10 mb for incident neutron energies between 2.5 and 4.5 MeV. These γ rays may produce interferences for a $0\nu\beta\beta$ signal at the Q value of 2458 keV as both lie within the current resolution of the EXO-200 detector (FWHM $\approx$ 100 keV) [7] for the neutrinoless double-β decay signature. Levels with energies within the ROI are also of importance as they produce cascades of γ rays, which may be detected as multisite events. The presented INS γ-ray production cross sections are important input for calculations to model the backgrounds that appear in the spectra and assist in the unambiguous identification of $0\nu\beta\beta$ events.

ACKNOWLEDGMENTS

This material is based upon work supported by the US National Science Foundation under Grant No. PHY-1606890. The authors wish to thank A. Pocar of the EXO-200 Collaboration for fruitful discussions leading to a deeper understanding of the operation of the EXO-200 experiment and the relevance of these cross section measurements. We also wish to thank H. E. Baber for his invaluable contributions to maintaining the UKAL.

[1] F. T. Avignone, S. R. Elliott, and J. Engel, Rev. Mod. Phys. **80**, 481 (2008).
[2] N. Abgrall *et al.* (Majorana Collaboration), Adv. High Energy Phys. **2014**, 365432 (2014).
[3] M. Agostini *et al.* (GERDA Collaboration), Nucl. Part. Phys. Proc. **273-275**, 1876 (2016).
[4] J. B. Albert *et al.* (EXO-200 Collaboration), Phys. Rev. C **89**, 015502 (2014).
[5] A. Gando *et al.* (KamLAND-Zen Collaboration), Phys. Rev. Lett. **117**, 082503 (2016).
[6] M. Wang, G. Audi, A. H. Wapstra, F. G. Kondev, M. MacCormick, X. Xu, and B. Pfeiffer, Chin. Phys. C **36**, 1603 (2012).
[7] M. Auger *et al.* (EXO-200 Collaboration), Phys. Rev. Lett. **109**, 032505 (2012).
[8] C. A. Engelbrecht, Nucl. Instrum. Methods **80**, 187 (1970).
[9] R. Beyer, R. Schwengner, R. Hannaske, A. R. Junghans, R. Massarczyk, M. Anders, D. Bemmerer, A. Ferrari, A. Hartmann, T. Kögler, M. Röder, K. Schmidt, and A. Wagner, Nucl. Phys. **A927**, 41 (2014).